

# Mass Transfer around a Rising CO<sub>2</sub> Bubble in an Air Lift Column Applied to Aquaculture

Djimako Bongo<sup>1\*</sup>, Edith Kadjagaba<sup>2</sup>, Nekoulngang Djetounako Clarisse<sup>2</sup>, Jean-Yves Champagne<sup>3</sup>

<sup>1</sup>National Institute of Science and Technology of Abéché, Abéché, Chad

<sup>2</sup>Faculty of Exact and Applied Sciences, University of N'Djamena, N'Djamena, Chad

<sup>3</sup>Laboratory of Fluid Mechanics and Acoustics INSA-Lyon, Lyon, France

Email: \*djimako.b5@gmail.com

**How to cite this paper:** Bongo, D., Kadjagaba, E., Clarisse, N.D. and Champagne, J.-Y. (2020) Mass Transfer around a Rising CO<sub>2</sub> Bubble in an Air Lift Column Applied to Aquaculture. *Natural Resources*, 11, 205-217.

<https://doi.org/10.4236/nr.2020.115013>

**Received:** March 14, 2020

**Accepted:** May 4, 2020

**Published:** May 7, 2020

Copyright © 2020 by author(s) and Scientific Research Publishing Inc.

This work is licensed under the Creative Commons Attribution International

License (CC BY 4.0).

<http://creativecommons.org/licenses/by/4.0/>



Open Access

---

## Abstract

He mentioned in the 18th century the possibility of injecting gas bubbles into a column of liquid to create a displacement of this liquid due to the rise of bubbles. This system takes the name of Air Lift and the first publications around this process appear at the beginning of the 20th century. There are many economic and ecological interests: CO<sub>2</sub> from industrial production is valued because it is consumed by algae, which once they reach maturity can be converted into fuel. It is therefore a very good energy balance thanks to a low consumption of gray energy and the system is simple to set up. In this study, we will delve deeper into the description of the bubble column and the theory that accompanies it. We will then describe our experiences and the work done.

## Keywords

Mass Transfer, PLIF, PIV, Transverse Velocity, CO<sub>2</sub>

---

## 1. Introduction

If the pumping of water with the help of air bubbles is quickly exploited, especially when it is necessary to create a flow in a liquid heavily loaded with particles, the process has found new applications that fit in sustainable development [1]. The bubble column is an answer to this problem because it presents itself as a multifunctional system [2] [3] [4]. It ensures the circulation of water, the bubbles of gas ensuring the pumping of the liquid and the gas exchange at the interface between the bubbles and the water make it possible to deplete the liquid in CO<sub>2</sub>. Small organic waste is driven by bubbles and can be recovered at the top of the column. The second application of the column lies in the culture of mi-

cro-algae. In fact, bio-fuels are one of the most important alternatives to fossil fuels. However, they face serious performance problems. The use of aquatic micro-algae as bio-fuels requires little arable land [5]. Rich in lipids, they can produce 100 to 300 times more fuel than palm oil [6]. Biomass production using captured CO<sub>2</sub> to produce biological hydrogen and to exploit the biomass to extract biomolecules or other biofuels. But the production of biocarbons is not a priority as our study focuses a lot on spirulina. The application of the airlift is of great interest in the production of micro-algae [7] coupled with a raceway basin [8], it provides the three functions necessary for the development and harvesting of micro-algae. The circulation of water by pumping and the enrichment in CO<sub>2</sub> of the culture by gas exchange at the interface of the bubbles then the harvest of the mature algae, driven by the bubbles, which will form a scum on the surface of the column [9] [10]. However, the analysis of the particle size of the bubbles in the columns is carried out by techniques intrusive, disrupting flow and by non-intrusive techniques [11]. Non-intrusive techniques use tomographic probes [11] [12] or PIV image analysis [13].

## 2. Description of the Experimental Bench

The column used as shown in **Figure 1** is a column polymethyl methacrylate (Plexiglas) whose dimensions are 25 × 25 × 70 cm with a constant wall thickness of 2 cm. Therefore, the capacity of the column is: 30.87 L. The column has a black plate on the underside, on which the injection system is connected as well as the various tools put in place during the realization of the experiments. The experimental bench set up at the LMFA laboratory is described in **Figure 1**. The gas used is respectively air for the PIV and CO<sub>2</sub> for the PLIF. This is injected into the tank containing deionized water (PLIF) [14] or different solutions of water plus glycerin (PIV) and fluorescein (PLIF) or crystals (PIV). The tank is then illuminated by the laser, the bubbles are visible in the laser plane and images can be recorded on the computer via the camera. Two probes are placed at the level of the tank to make measurements of CO<sub>2</sub> concentration and pH (PLIF).

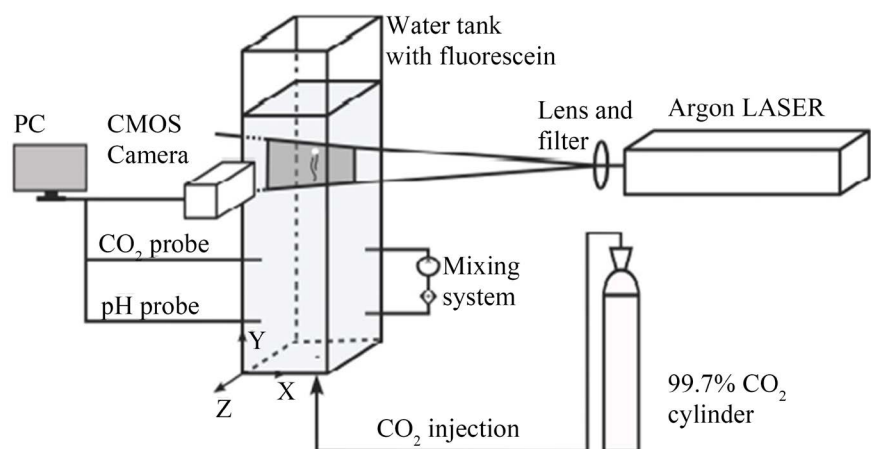


**Figure 1.** The experience bench.

## 2.1. Operation

PIV (Particle Image Velocimetry) measures a complete velocity field using short interval images [15] [16]. This technique can be used to study a gas or a liquid. PLIF (Planar Laser-Induced Fluorescence) is a technique widely used in the study of fluids. This technique makes it possible to observe the flows but also the fields of concentration and temperature in a two-phase flow. The luminous excitation of fluorescein and crystals is done using a Laser Argon (Light Amplification by Stimulated Emission of Radiation) **Figure 2**. This Laser was chosen because it is capable of emitting at several lengths of wave between 457.9 - 514.5 nm. Fluorescein as the crystals are excited at about 500 nm, wavelength corresponding to the blue-cyan color, a filter is placed at the output of the laser beam to have only one wavelength emitted on the tank [17]. However, this filter will lose 80% - 90% of the power of the Laser, but it does not prevent the fluorescein and the crystals are excited because one of the ideas used to solve this problem is to place a reflective mirror at opposite side of the Laser to double the power output. Note also that the Laser must be cooled due to a large heat emission during operation. The flow rate of the cooling system is adjusted to around 10 L/min, thus avoiding instability of power and temperature. The normal power of use of the Laser rotates around 8 W. The intensity can be adjusted to optimize the exposure time at the camera and to have better images.

## 2.2. Protocol

In order to study the behavior of bubbles in different solutions, we chose to take images with different flow rates and needle diameters for four glycerin concentrations. In our experiments, three different types of diameter were used:  $\varnothing 0.8$  mm;  $\varnothing 0.6$  mm;  $\varnothing 0.4$  mm. For PIV, Dantec dynamics particles were used. These particles are spherical crystals HGS-10, Hollow  $\varnothing 10$   $\mu\text{m}$ . They are used at a wavelength around 500  $\mu\text{m}$ . Four 20 L solutions were used in our experiments, which are defined by their glycerin percentage by volume. For the demineralized water solution and for the 20% solution of glycerin, solutions with a low viscosity,

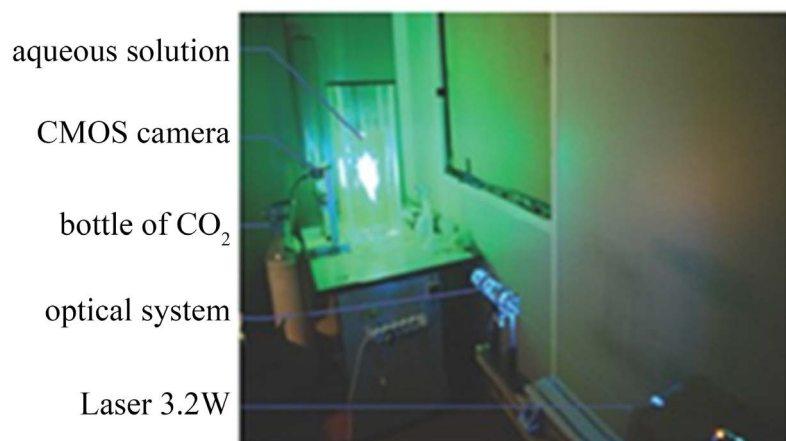


**Figure 2.** Laser bubble column.

we find that the rise of the bubbles takes a spiral trajectory (3D) **Figure 3** when injecting low flow rates. On the other hand, the bubbles rotate about themselves and each of them has its own trajectory. For solutions of 30% and 40% glycerin we can notice that the rise of the bubbles follows a zigzag trajectory but in the case of the solution 30%, this trajectory is in 2D **Figure 3** whereas for the solution 40% it is in 3D and less marked (**Figure 4**). In this last case, we can also see

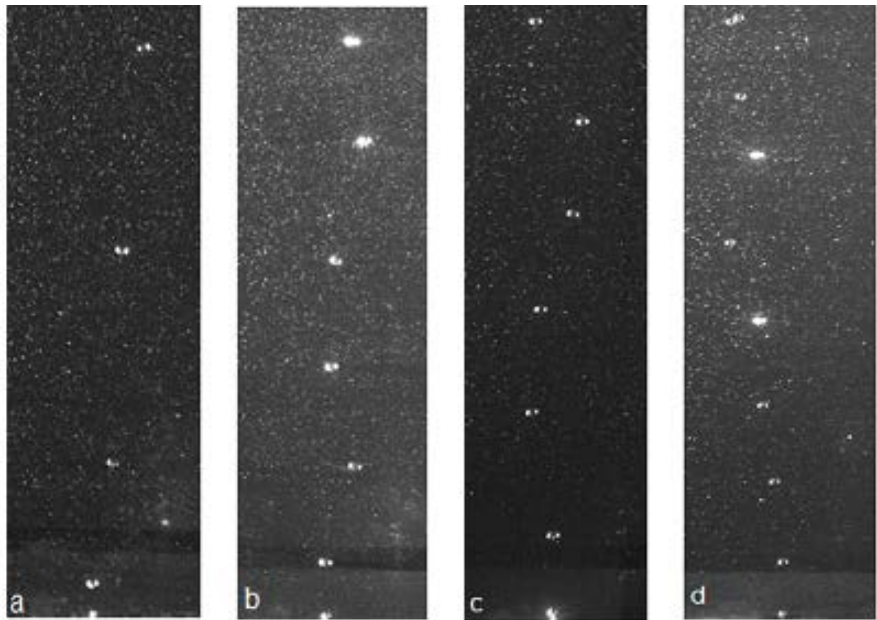


**Figure 3.** Photos of the trajectories of the bubbles ((a) Demineralized water, (b) 20% solution of glycerin, (c) Solution with 30% of glycerin, (d) Solution with 40% of glycerin).

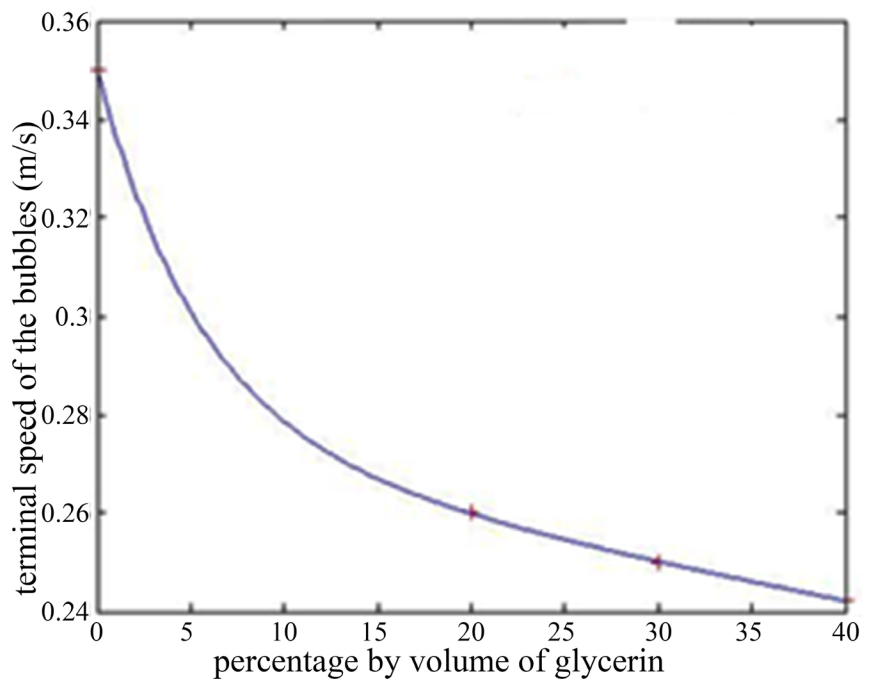


**Figure 4.** Terminal velocity versus glycerin concentration.

that the upstream bubble crashes against the downstream bubble, the one coming out of the plane in which it was and can follow a new trajectory with a different speed. The terminal velocities in **Figure 4** have been calculated. It is noted that this decreases exponentially, the higher the concentration of glycerin increases.

### 2.3. Fluorescein

In order to study the dissolution of  $\text{CO}_2$ , we use fluorescein. Indeed, when the concentration of  $\text{CO}_2$  increases, the pH decreases and the re-emission of fluorescein photons also appears in **Figure 5**. Fluorescein is a dye which has the particularity of returning a fluorescent light when it is excited at a wavelength of 494 nm [18].

It is observed that the maximum is reached is reached at around 5.10 - 7 mol/L (**Figure 6**). For a water depth of 40 cm or 18 L, we used 100 mL of fluorescein at a concentration of 0.034 g/L. In order to exploit PLIF results, it is necessary to make a calibration. Thus, a series of images is produced at different concentrations and the corresponding light intensity and the pH are measured. It is therefore possible to obtain curves that bind the pH, the light intensity and the  $\text{CO}_2$ .

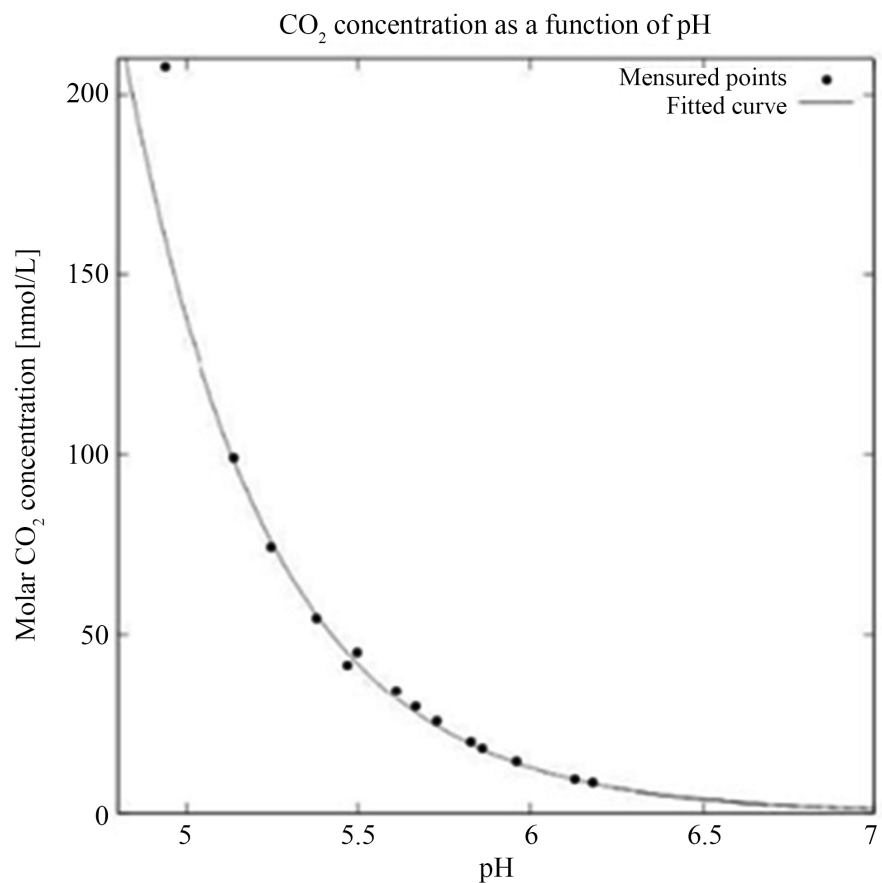


**Figure 5.** CO<sub>2</sub> concentration as a function of pH.

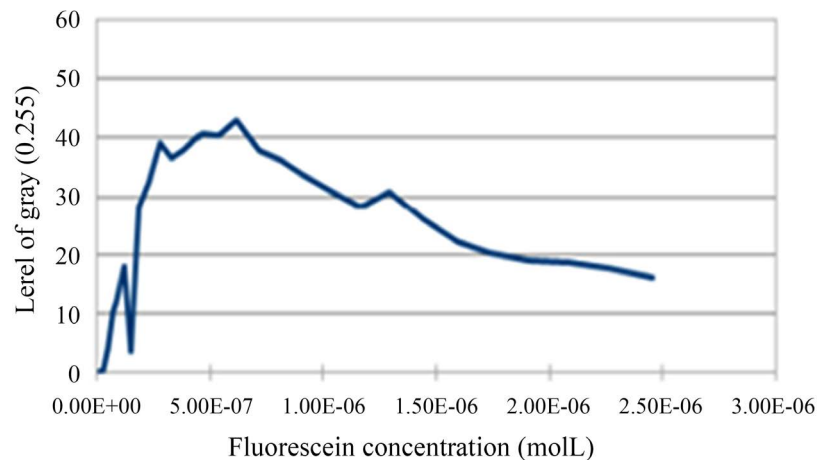


**Figure 6.** Light intensity versus fluorescein concentration.

## 2.4. Settings

- Camera: Exposure time: 2500  $\mu$ s, Frequency: 206 FPS, Image size: 1399  $\times$  500, Dynamic gain: 3000 DN
- Particles: When brightness is high, it is best to use 10  $\mu$ m glass particles. In the case of a lack of brightness, polyamide particles of 50  $\mu$ m are used.
- Pump flow syringe: 100
- Needle diameters:  $\varnothing$ 0.4;  $\varnothing$ 0.6 and  $\varnothing$ 0.8.
- Column filled up to 40 cm with 17.96l of demineralized water and 0.1l of fluorescein.
- Gas: 99.9% CO<sub>2</sub> of liquid air.

## 3. Results

### 3.1. Average Speed Fields

**Figure 7** shows the average speed fields. These measurements were taken for air flow rates equal to  $Q_{60} = 2.548 \text{ cm}^3/\text{min}$  and a  $\varnothing$ 0.8 mm.

Note that the average displacement value of the liquid in the column is a function of the viscosity of the liquid used. Indeed, for a fairly viscous liquid (40% glycerin) the speed undergoes an increase of about 50% compared to that of pure water.

### 3.2. Cross-Sectional Velocity Profiles

In order to characterize the distribution of the velocity field in the whole of the studied volume, the transverse profiles in different planes of the column were determined (**Figures 8-11**). The results show that these profiles are more and more flattened by decreasing the viscosity. This is mainly due to the value of the volume density of the liquid which increases as a function of the viscosity and consequently the displacement of the gas bubbles cannot cause a displacement on the totality of the liquid contained in the column. It is for this reason that we notice quite significant speeds around the central axis of the column for the most viscous solution.

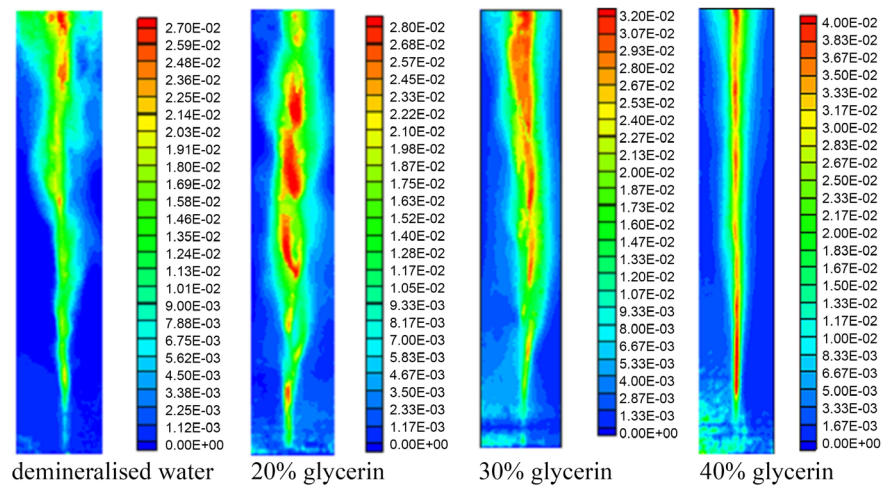


Figure 7. Average speed field of the different solutions.

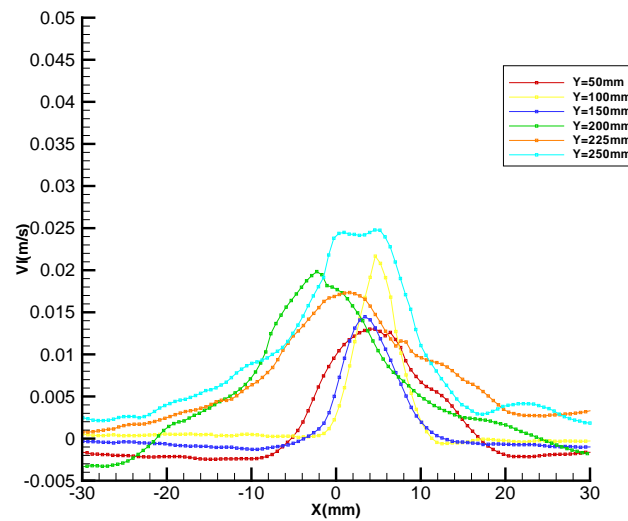


Figure 8. Transverse velocity profiles for demineralized water.

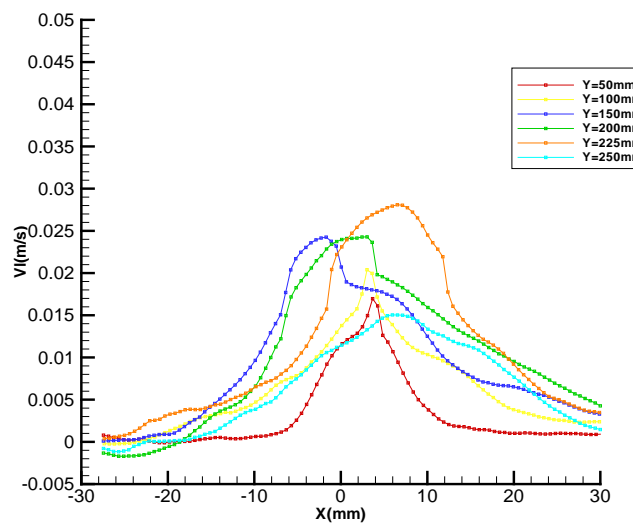
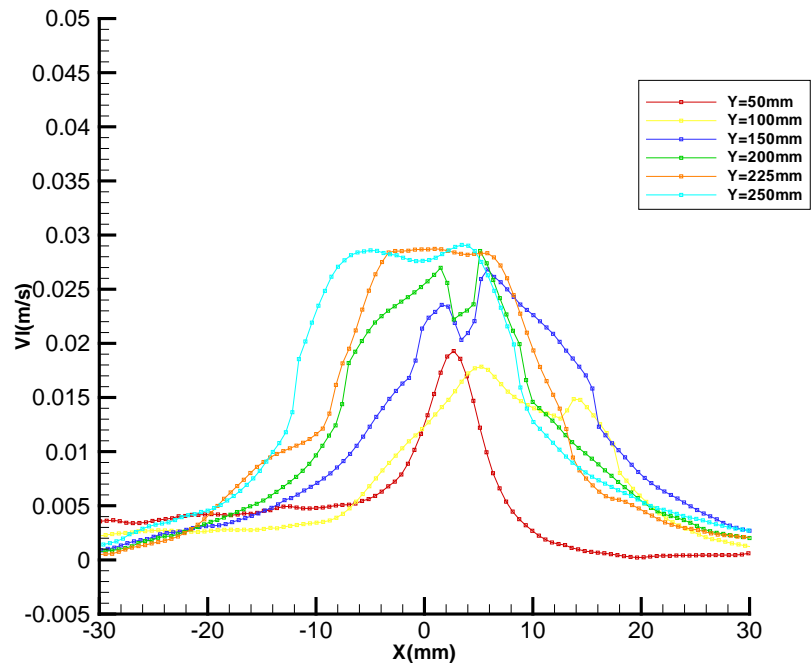
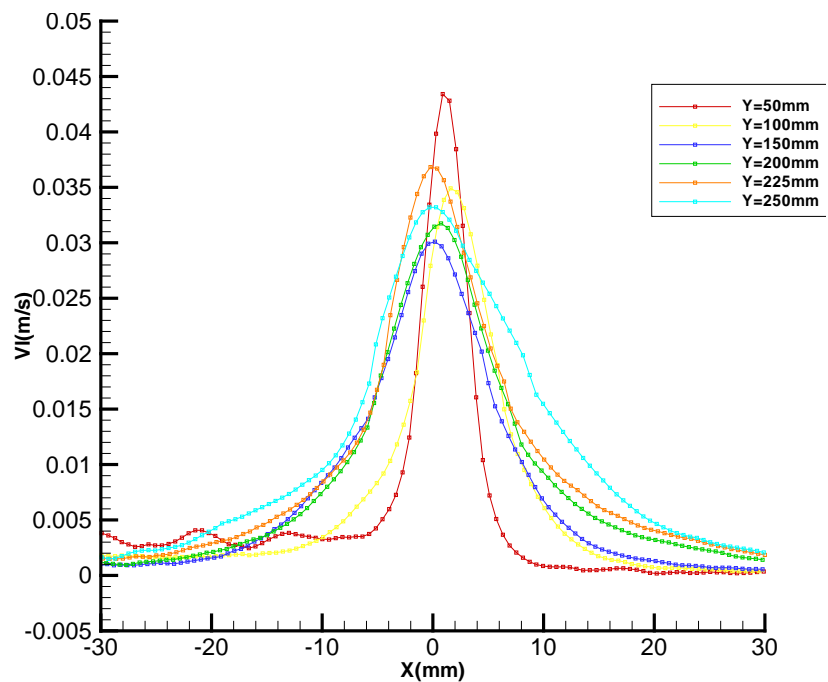


Figure 9. Cross-sectional velocity profiles for 20% glycerin.



**Figure 10.** Transverse velocity profiles for 30% glycerin.



**Figure 11.** Transverse velocity profiles for 40% glycerin.

In **Figure 4**, it was noted that bubble velocities decreased as glycerin concentration increased. However, when we observe the transverse velocity profiles, we notice that the velocity of the fluid increases with the concentration of glycerin. This is because the slip speed decreases with increasing glycerin concentration. As a result, the fluid is more driven by the bubble when there is viscosity, which explains the higher fluid speeds.

### 3.3. Image Processing

For lack of time we could not take quality picture series for all needles. However, the programs are now functional and the protocol is clearly established. Here is the result for a  $\varnothing 0.6$  mm needle. The MATLAB program processes only one image. Here are the results of the different stages of treatment. **Figure 12** shows the raw image of the PLIF and PIV and **Figure 13** shows the velocity field result processed but **Figure 16** shows the superimposed result PIV-PLIF deals with Davis 8.1.

The particularity of our work is the use of a doubler to acquire PIV and PLIF. This allowed us to follow the dissolution of  $\text{CO}_2$ , determine its concentration field, and then visualize the velocity profiles. But also to superimpose the two images PIV and PLIF.

During our work, we found that at  $t = 0$ , there is no bubble on the water table **Figure 14(a)**, but at  $t = 0.30$  s we observe the first bubble on the water table then at  $0.43$  s it goes out of the Laser Plan **Figure 14(b)**.

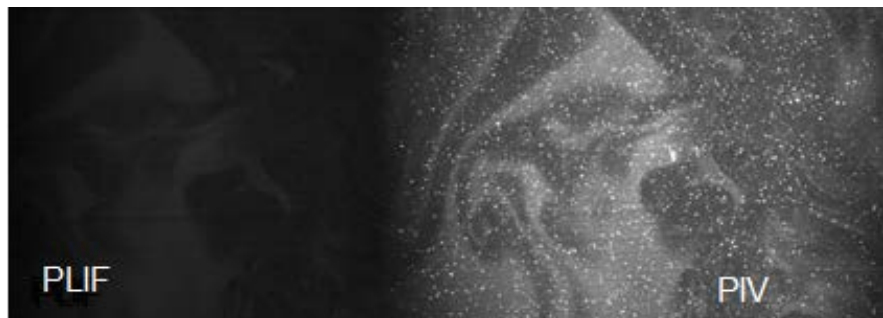


**Figure 12.** Initial image PLIF-PIV.

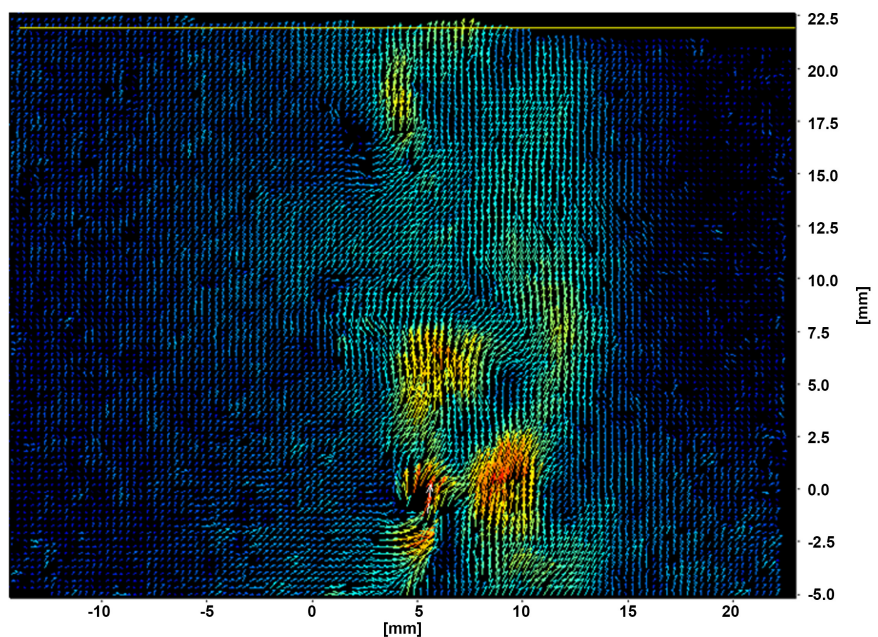


**Figure 13.** Davis PIV result.

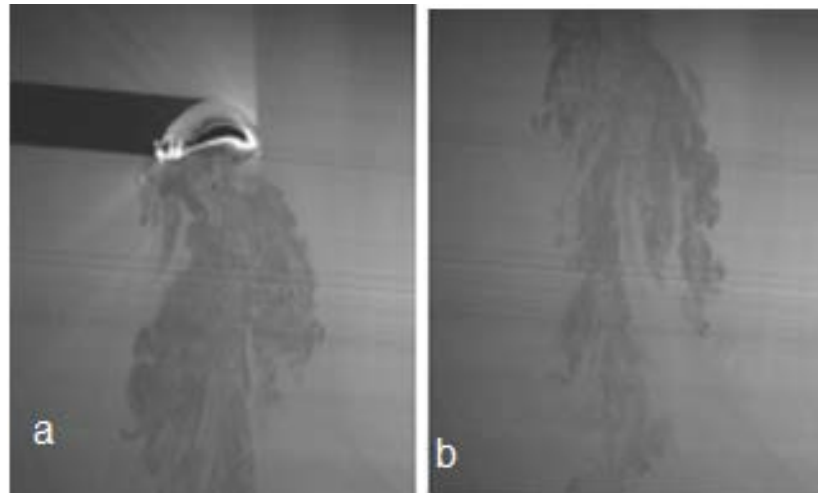


**Figure 14.** Image of the acquisition.

Bubble columns have long been used in water treatment to capture different types of particles. More recently, it is their exchange capacity that has been used to produce chemical reactions between gas phase and liquid phase [13]. The vacuum bubble column studied dissolves carbon dioxide in water (Figure 14 and Figure 15) [7]. This carbon-rich water is an ideal medium for growing micro-algae. The production of these micro-algae is today an issue in many fields since it can be intended for medicinal, food or energy use in the form of biofuel. It is therefore important to understand the phenomena and parameters at stake before scaling up (Figure 16).

These theoretical results of PLIF and PIV will be applied to the culture of a blue-green algae: *Spirulina Platensis*. The choice of this plant-bacterium is based on several criteria: short culture cycle, applications in cosmetics, medicine and high nutritional value. Thus, we were able to study the influence of culture parameters such as light intensity,  $\text{CO}_2$  velocity and concentration field, and temperature on its growth. In addition, we have implemented two methods based on bubble velocity and  $\text{CO}_2$  dissolution to quantify the biomass produced by spirulina.

#### 4. Conclusion

Despite the age of the airlift technology, it has not found applications in the industrial field, particularly in the fields of seaweed farming and fish farming. They prove the effectiveness of the column as a multi-functional system able to both manage the circulation of water [19], the injection and removal of dissolved solids and the recovery of suspended solids. The work devoted to the transfer of the gas-liquid mass, by means of the PLIF and PIV method, the dissolution of the  $\text{CO}_2$  could be quantified in the bubble column, the field of concentration and velocity showing a great efficiency of this one to dissolve carbon dioxide [20]. The size of the bubbles has a very strong influence on the efficiency of the air lift. The study of bubble sizes according to natures of water could show the importance

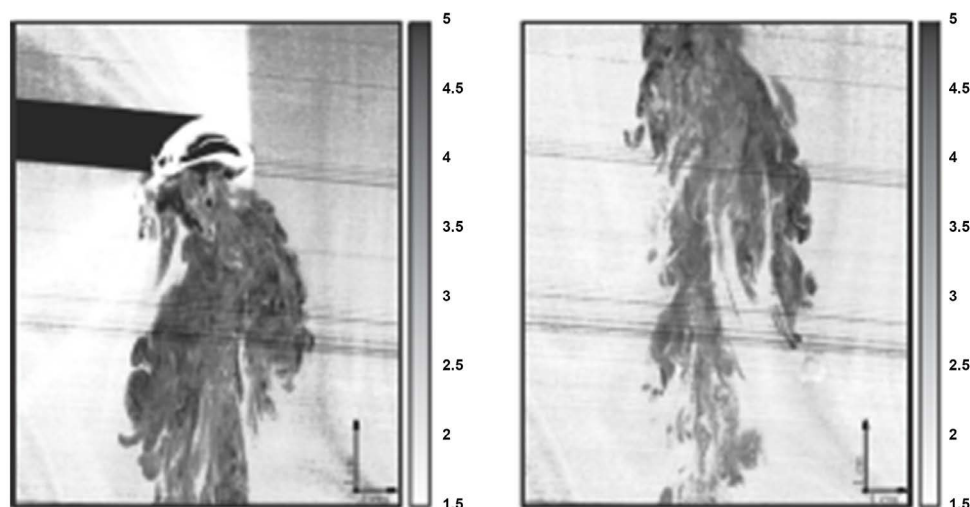


**Figure 15.** Concentration of CO<sub>2</sub> treated with Davis.

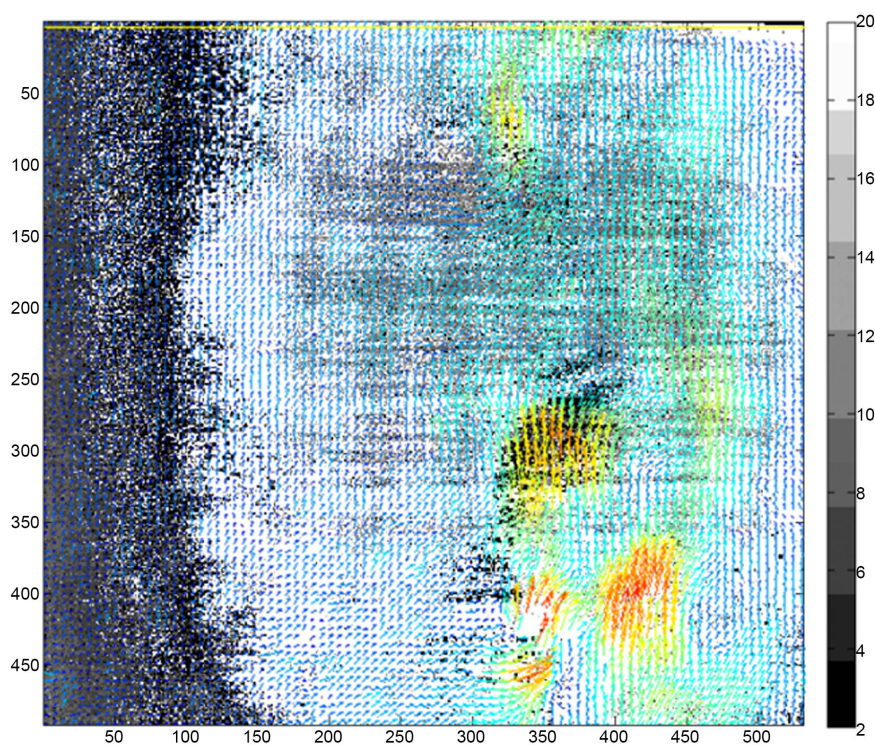


**Figure 16.** Superimposed PIV and PLIF images.

of operating the column in demineralized water or with a glycerin percentage not exceeding 40%. In fact, the bubbles are much smaller than in demineralized water than in water containing glycerin, and therefore the gas-liquid exchange surface is larger.

### Conflicts of Interest

The authors declare no conflicts of interest regarding the publication of this paper.

## References

- [1] Aljerf, L. and Choukaife, A.E. (2016) Sustainable Development in Damascus University: A Survey of Internal Stakeholder Views. *Journal of Environmental Studies*, **2**, 1-12. <https://doi.org/10.13188/2471-4879.1000012>
- [2] Barrut, B. (2011) Etude et optimisation du fonctionnement d'une colonne airlift à dépression—Application à l'aquaculture. 137 p.
- [3] Barru, B., *et al.* (2011) Mass Transfer Efficiency of a Vacuum Airlift—Application to Water Recycling in Aquaculture Systems. *Aquacultural Engineering*, **46**, 18-26. <https://doi.org/10.1016/j.aquaeng.2011.10.004>
- [4] Jacquety, J. (2007) Etude d'un système innovant et multifonctionnel de traitement de l'eau en circuit recirculé. Rapport de fin d'études DESTA, Intechmer/Cnam. DESTA/2007/07.
- [5] Hannon, M., Gimpel, J., Tran, M., Rasala, B. and Mayfield, S. (2010) Biofuels from Algae: Challenges and Potential. *Biofuels*, **1**, 763-784. <https://doi.org/10.4155/bfs.10.44>
- [6] Aljerf, L. (2015) Fabrication et test d'un catalyseur d'acide sulfonique approprié pour la réaction de production des biocarburants. *Afrique Science*, **11**, 349-358.
- [7] Mazzuca Sobczuk, T., Garcya Camacho, F., Camacho Rubio, F., Acien Fernandez, F.G. and Molina Grima, E. (1999) Carbon Dioxide Uptake Efficiency by Outdoor Microalgal Cultures in Tubular Airlift Photobioreactors. *Biotechnology and Bioengineering*, **67**, 465-475. [https://doi.org/10.1002/\(SICI\)1097-0290\(20000220\)67:4<465::AID-BIT10>3.0.CO;2-9](https://doi.org/10.1002/(SICI)1097-0290(20000220)67:4<465::AID-BIT10>3.0.CO;2-9)
- [8] Bongo, D., *et al.* (2016) Amélioration du rendement de la culture des microalgues par la désaturation du dioxyde de carbone. *Afrique Science*, **12**, 43-50.
- [9] Teng, H., Masutani, S.M., Kinoshita, C.M. and Nihous, G.C. (1996) Solubility of CO<sub>2</sub> in the Ocean and Its Effect on CO<sub>2</sub> Dissolution. *Energy Conversion and Management*, **37**, 1029-1038. [https://doi.org/10.1016/0196-8904\(95\)00294-4](https://doi.org/10.1016/0196-8904(95)00294-4)
- [10] Lucchetti, A. (2014) Modélisation et conception d'un système de culture de microalgues. Thèse, 107-114.
- [11] Adetunji, O. and Rawatlal, R. (2016) Estimation of Bubble Column Hydrodynamics: Image-Based Measurement Method. *Flow Measurement and Instrumentation*, **53**, 4-17. <https://doi.org/10.1016/j.flowmeasinst.2016.08.002>
- [12] Young, M.A., *et al.* (1991) Airlift Bioreactors: Analysis of Local Two Phase Hydrodynamics. *AIChE Journal*, **37**, 403-428. <https://doi.org/10.1002/aic.690370311>
- [13] Chaumat, H., *et al.* (2007) On the Reliability of an Optical Fibre Probe in Bubble Column under Industrial Relevant Operating Conditions. *Experimental Thermal and Fluid Science*, **31**, 495-504. <https://doi.org/10.1016/j.exptthermflusci.2006.04.018>
- [14] Muhlriedel, K. and Baumann, K.H. (2000) Concentration Measurements during Mass Transfer across Liquid-Phase Boundaries Using Planar Laser Induced Fluorescence (PLIF). *Experiments in Fluids*, **28**, 279-281. <https://doi.org/10.1007/s003480050388>
- [15] Lyn, D.A. (1997) A PIV Study of an Oscillating-Grid Flow. *Experimental and Numerical Flow Visualization and Laser Anemometry*, Vol. 13, Fluids Engineering Division (Publication). ASME, New York.
- [16] Besbes, S., *et al.* (2015) PIV Measurements and Eulerian-Lagrangian Simulations of the Unsteady Gas-Liquid Flow in a Needle Sparger Rectangular Bubble Column. *Chemical Engineering Science*, **126**, 560-572.

<https://doi.org/10.1016/j.ces.2014.12.046>

- [17] Valiorgue, P., Souzy, N., El Hajem, M., Ben Hadid, H. and Simoens, S. (2012) PLIF Treatment Method for a Non-Optically Thin Experimental Setup. 14 p.
- [18] Walker, D. (1987) A Fluorescence Technique for Measurement of Concentration in Mixing Liquids. *Journal of Physics: Scientific Instruments*, **20**, 217.  
<https://doi.org/10.1088/0022-3735/20/2/019>
- [19] Besagni, G., *et al.* (2017) The Dual Effect of Viscosity on Bubble Column Hydrodynamics. *Chemical Engineering Science*, **158**, 509-538.  
<https://doi.org/10.1016/j.ces.2016.11.003>
- [20] Spycher, N., Pruess, K. and Ennis-King, J. (2003) CO<sub>2</sub>-H<sub>2</sub>O Mixtures in the Geological Sequestration of CO<sub>2</sub>. I. Assessment and Calculation of Mutual Solubilities from 12 to 100 °C and Up to 600 Bar. *Geochimica et Cosmochimica Acta*, **67**, 3015-3031.  
[https://doi.org/10.1016/S0016-7037\(03\)00273-4](https://doi.org/10.1016/S0016-7037(03)00273-4)